SIP/CacyBP promotes autophagy by regulating levels of BRUCE/Apollon, which stimulates LC3-I degradation

Tian-Xia Jiang[a,1], Jiang-Bo Zou[a,1], Qian-Qian Zhu[a,1], Cui Hua Liu[b,1], Guang-Fei Wang[a,1], Ting-Ting Du[a,1], Zi-Yu Luo[a], Fang Guo[a], Lu-Ming Zhou[a], Juan-Juan Liu[a], Wensheng Zhang[c], You-Sheng Shu[d], Li Yu[e], Peng Li[e], Ze'ev A. Ronai[f], Shu-ichi Matsuzawa[g], Alfred L. Goldberg[h,2], and Xiao-Bo Qiu[a,2]

[a]State Key Laboratory of Cognitive Neuroscience & Learning and Ministry of Education Key Laboratory of Cell Proliferation & Regulation Biology, College of Life Sciences, Beijing Normal University, 100875 Beijing, China; [b]Chinese Academy of Sciences Key Laboratory of Pathogenic Microbiology and Immunology, Institute of Microbiology, Chinese Academy of Sciences, 100101 Beijing, China; [c]Beijing Area Major Laboratory of Protection and Utilization of Traditional Chinese Medicine, Beijing Normal University, 100875 Beijing, China; [d]State Key Laboratory of Cognitive Neuroscience & Learning, School of Brain and Cognitive Sciences, Beijing Normal University, 100875 Beijing, China; [e]School of Life Sciences, Tsinghua University, 100084 Beijing, China; [f]Cancer Center, Sanford Burnham Prebys Medical Discovery Institute, La Jolla, CA 92037; [g]Department of Neurology, Kyoto University Graduate School of Medicine, 606-8507 Kyoto, Japan; and [h]Department of Cell Biology, Harvard Medical School, Boston, MA 02215

Contributed by Alfred L. Goldberg, May 15, 2019 (sent for review January 22, 2019; reviewed by Ana Maria Cuervo and Keiji Tanaka)

BRUCE/Apollon is a membrane-associated inhibitor of apoptosis protein that is essential for viability and has ubiquitin-conjugating activity. On initiation of apoptosis, the ubiquitin ligase Nrdp1/RNF41 promotes proteasomal degradation of BRUCE. Here we demonstrate that BRUCE together with the proteasome activator PA28γ causes proteasomal degradation of LC3-I and thus inhibits autophagy. LC3-I on the phagophore membrane is conjugated to phosphatidylethanolamine to form LC3-II, which is required for the formation of autophagosomes and selective recruitment of substrates. SIP/CacyBP is a ubiquitination-related protein that is highly expressed in neurons and various tumors. Under normal conditions, SIP inhibits the ubiquitination and degradation of BRUCE, probably by blocking the binding of Nrdp1 to BRUCE. On DNA damage by topoisomerase inhibitors, Nrdp1 causes monoubiquitination of SIP and thus promotes apoptosis. However, on starvation, SIP together with Rab8 enhances the translocation of BRUCE into the recycling endosome, formation of autophagosomes, and degradation of BRUCE by optineurin-mediated autophagy. Accordingly, deletion of SIP in cultured cells reduces the autophagic degradation of damaged mitochondria and cytosolic protein aggregates. Thus, by stimulating proteasomal degradation of LC3-I, BRUCE also inhibits autophagy. Conversely, SIP promotes autophagy by blocking BRUCE-dependent degradation of LC3-I and by enhancing autophagosome formation and autophagic destruction of BRUCE. These actions of BRUCE and SIP represent mechanisms that link the regulation of autophagy and apoptosis under different conditions.

CacyBP/SIP | BRUCE/Apollon | LC3 | autophagy | apoptosis

The balance between proapoptotic and antiapoptotic proteins is critical for normal development, for the proper functioning of many tissues postnatally, and in the pathogenesis of various diseases, especially cancer (1, 2). Normally, apoptosis is inhibited by the inhibitor of apoptosis protein (IAP) family. The only essential IAP is the exceptionally large (~530 kDa) membrane-associated protein BRUCE/Apollon, which has a ubiquitin-conjugating (E2) domain. BRUCE can inhibit apoptosis by serving as both E2 and E3 (i.e., ubiquitin ligase) for the ubiquitination of key proapoptotic proteins, especially caspases and SMAC/DIABLO (3–6). On initiation of apoptosis, the ubiquitin ligase Nrdp1/RNF41 promotes ubiquitination and degradation of BRUCE, apparently by the 26S proteasome (6). This large proteolytic complex degrades the great majority of cell proteins, which are marked for selective destruction by attachment of a chain of ubiquitin molecules (7).

The other major intracellular system for degrading cell proteins is macroautophagy (referred to below as autophagy), in which cytosolic proteins and organelles are engulfed in membrane-enclosed structures termed autophagosomes (8, 9). Some ubiquitinated proteins are degraded by autophagy after binding to ubiquitin receptors, such as p62/SQSM1 and optineurin (OPTN), which then bind to the LC3/GABARAP/ATG8 family of proteins on the autophagosome membrane (10). Present on both the outer and inner membranes of the autophagosome are members of the LC3/GABARAP/ATG8 family of proteins. In mammals, there are 2 subfamilies of these proteins, of which LC3B is the most prevalent and is the precursor of LC3-I and LC3-II. LC3B is cleaved by ATG4 to form cytoplasmic LC3-I. This protein is then conjugated to phosphatidylethanolamine on the phagophore membrane to form LC3-II. LC3-II is required not only for autophagosome biogenesis, but also for selective recruitment of substrates into the autophagosome (8, 9).

The present study identifies several factors that regulate rates of apoptosis as well as autophagy through effects on LC3-I content. SIP/CacyBP (Siah1-interacting protein/calcyclin-binding protein) is a ubiquitous protein that is highly expressed in neurons and is up-regulated in certain tumors (11). It has been implicated in the ubiquitination and proteasomal degradation of β-catenin, an oncogenic protein that normally regulates cell adhesion and gene

Significance

BRUCE/Apollon is an unusual inhibitor of apoptosis protein containing a ubiquitin-conjugating domain. Here we show that BRUCE is also an inhibitor of autophagy by promoting the proteasomal degradation of LC3-I, the precursor of LC3-II, which is critical in autophagosome biogenesis and substrate recruitment. SIP/CacyBP, which is highly expressed in neurons and various tumors, promotes autophagy by enhancing autophagic degradation of BRUCE and promoting autophagosome formation. DNA damage by the anticancer agents camptathecin and etoposide caused monoubiquitination of SIP by the ubiquitin ligase Nrdp1 and stimulated apoptosis. Deletion of SIP reduced the autophagic degradation of BRUCE and damaged mitochondria. This study identifies unanticipated mechanisms that regulate both autophagy and apoptosis, whose roles in physiology and disease will be important to investigate.

Author contributions: T.-X.J., J.-B.Z., Q.-Q.Z., C.H.L., G.-F.W., and T.-T.D. designed research; T.-X.J., J.-B.Z., Q.-Q.Z., C.H.L., G.-F.W., and T.-T.D. performed research; T.-X.J., J.-B.Z., Q.-Q.Z., C.H.L., G.-F.W., T.-T.D., Z.-Y.L., F.G., L.-M.Z., J.-J.L., W.Z., Y.-S.S., L.Y., P.L., Z.A.R., S.-i.M., A.L.G., and X.-B.Q. analyzed data; and A.L.G. and X.-B.Q. wrote the paper.

Reviewers: A.M.C., Albert Einstein College of Medicine; and K.T., The Tokyo Metropolitan Institute of Medical Science.

The authors declare no conflict of interest.

[1]T.-X.J., J.-B.Z., Q.-Q.Z., C.H.L., G.-F.W., and T.-T.D. contributed equally to this work.

[2]To whom correspondence may be addressed. Email: Alfred_Goldberg@hms.harvard.edu or xqiu@bnu.edu.cn.

This article contains supporting information online at www.pnas.org/lookup/suppl/doi:10.1073/pnas.1901039116/-/DCSupplemental.

Published online June 18, 2019.

transcription (12). We show here that BRUCE, along with being an IAP, is also an inhibitor of autophagy that promotes LC3-I degradation. Surprisingly, this process also requires the proteasome activator PA28γ, which binds to the ends of the 20S proteasome and has been implicated in ubiquitin-independent proteasomal degradation of certain proteins (13). We further show that SIP opposes the inhibition of autophagy by BRUCE, and that DNA damage by topoisomerase inhibitors activates SIP and thus promotes degradation of BRUCE and eventually apoptosis. Accordingly, the loss of SIP reduces autophagosome formation and decreases the autophagic degradation of BRUCE, mitochondria, and protein aggregates.

Results

Promotion of LC3-I Degradation by BRUCE. After fusion of the autophagosome with the lysosome, LC3-II is degraded together with the contents of the autophagosome (8). To examine the degradation pathways for LC3-I, we treated HEK 293T cells and mouse embryonic fibroblasts (MEFs) with the specific proteasome inhibitor bortezomib and found that this treatment markedly increased the levels of both LC3-I and LC3-II (*SI Appendix*, Fig. S1 *A* and *B*). When translation was blocked by cycloheximide (CHX), the degradation of LC3-II was attenuated by the lysosome inhibitor chloroquine, as expected, but also by bortezomib. In contrast, the degradation of LC3-I, but not LC3-II, was inhibited only by bortezomib (Fig. 1*A* and *SI Appendix*, Fig. S1 *C* and *D*). The effect of bortezomib on LC3-I was further confirmed in the Atg5-deficient MEFs, where LC3-II was absent (14) (Fig. 1*B*). These inhibitors did not inhibit the transcription of LC3 (*SI Appendix*, Fig. S1*E*). These results indicate that LC3-I, unlike LC3-II, is degraded by the proteasome rather than by the lysosome. Because LC3-II is derived from LC3-I (8), the bortezomib-induced increase in LC3-II level is probably an indirect effect caused by the accumulation of LC3-I following the inhibition of its degradation.

The LC3-interacting proteins usually contain a LC3-interacting region (LIR) with the consensus sequence, $X_{-3}X_{-2}X_{-1}[W/F/Y]X_1X_2[L/I/V]X_4X_5$, where alternative letters are placed in square brackets with a slash between them (15). A putative LIR motif is also present in BRUCE (amino acids 4673-TSS FLQV LV-4681 in mouse; Fig. 1*C*). To examine its role, we carried out coimmunoprecipitation and GST-pulldown experiments, which revealed that BRUCE bound LC3-I, but not LC3-II, directly via this LIR motif (Fig. 1*D* and *SI Appendix*, Fig. S1*F*). Furthermore, mutations at F4676A and V4679A in the proposed LIR motif of BRUCE reduced its interaction with LC3-I (Fig. 1F and *SI Appendix*, Fig. S1*G*). Of note, the LC3-I pulled down with BRUCE seemed to migrate faster than the LC3-I in the input, raising the possibility that BRUCE might preferentially associate with a trimmed or modified version of LC3-I. Because the anti-LC3 antibody (Sigma-Aldrich; catalog no. L7543) might also recognize the precursor of LC3-I (i.e., LC3B), we could not yet distinguish whether there is a specific pool of LC3-I targeted for proteasomal degradation.

To determine whether BRUCE controls the levels of LC3, thereby possibly regulating autophagy, we infected MEFs with the lentivirus encoding siRNA for BRUCE. At 3 d and 7 d after infection, knockdown of BRUCE increased the levels of both LC3-I and LC3-II. However, caspase 3 activation, a sign of apoptosis (16), was detected only at 7 d after infection (Fig. 1*E*). The knockdown of BRUCE by siRNA oligos also increased the levels of both LC3-I and LC3-II (*SI Appendix*, Fig. S1*H*). Accordingly, in a CHX chase experiment, BRUCE knockdown was found to attenuate the degradation of LC3-I as well as its homolog, GABARAP (Fig. 1*G* and *SI Appendix*, Fig. S1*I*). Knockdown of BRUCE also increased the formation of autophagosomal LC3-II puncta in HeLa cells (Fig. 1*H*). These findings strongly suggest that BRUCE promotes degradation of LC3-I by directly binding LC3-I via its LIR motif. Because LC3-II content is an indicator of the amount of autophagosome formation (9), these results (and results described below) also suggest that decreasing BRUCE levels promotes autophagy, even though the prolonged depletion of BRUCE eventually causes apoptosis.

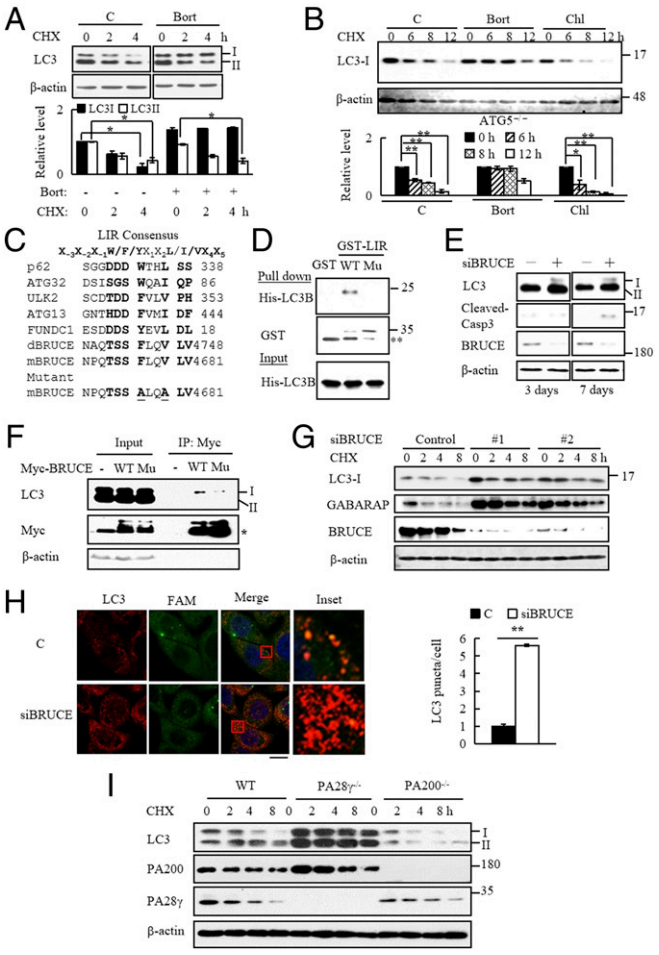

Fig. 1. BRUCE promotes the proteasomal degradation of LC3-I. (*A*) Degradation of LC3 in 293T cells treated with 25 μg/mL CHX for the indicated time and/or 100 nM bortezomib (Bort) for 12 h. (*B*) Degradation of LC3-I in the Atg5$^{-/-}$ MEFs treated with 100 nM Bort or 20 μM chloroquine (Chl) for 12 h in the presence of 25 μg/mL CHX for the time indicated. (*C*) The core LIR consensus sequence, $X_{-3}X_{-2}X_{-1}[W/F/Y]\ X_1X_2[L/I/V]X_4X_5$, where alternative letters are placed in square brackets with a solidus between them. (*D*) GST pulldown of His-tagged LC3B with the WT or mutant (Mu) LIR motif of BRUCE (amino acids 4623–4722), which was fused with GST. Double asterisks denote the free form of GST. (*E*) Knockdown of BRUCE in MEFs infected with lentivirus encoding siRNA for BRUCE for 3 or 7 d. (*F*) Coimmunoprecipitation of LC3-I with Myc-BRUCE in 293T cells transfected with the vector encoding the WT or mutant (Mu) BRUCE with a Myc tag. The asterisk denotes a nonspecific band. (*G*) The slowed degradation of LC3-I and GABARAP levels by knockdown of BRUCE in the Atg5$^{-/-}$ MEFs transfected with 2 pairs of siRNA oligos for BRUCE in the presence of 25 μg/mL of CHX. (*H*) Autophagosomal LC3 in HeLa cells transfected with siRNA oligos for BRUCE, which were fluorescently labeled with 6-FAM. LC3-II–containing autophagosomes were visualized by immunostaining. $n = 20$ images (Scale bar: 10 μm.) (*I*) Degradation of LC3-I in WT, PA28γ$^{-/-}$, and PA200$^{-/-}$ MEFs following treatment with 25 μg/mL CHX for the periods of time as indicated. Protein levels were analyzed by immunoblotting, and data are representative of 1 experiment with 2 independent biological replicates. LC3-I was detected with an anti-LC3 antibody (Sigma-Aldrich; catalog no. L7543), which might recognize LC3B as well. Data are mean ± SEM, representative of 1 experiment with 2 independent biological replicates. *$P < 0.05$; **$P < 0.01$, 2-tailed unpaired *t* test.

The members of the LC3/GABARAP/ATG8 family are highly homologous (17, 18). Therefore, we tested whether BRUCE

CELL BIOLOGY

associates with all the family members using GST-pulldown experiments and BRUCE's LIR motif (*SI Appendix*, Fig. S2*A*). The strongest interaction was between BRUCE and LC3B, although the LIR motif of BRUCE also weakly bound to 3 other family members, GABARAP, GABARAPL1 and GABARAPL2. Surprisingly, LC3B2, which differs from LC3B in only one amino acid (C113Y), showed almost no association with the LIR motif of BRUCE (*SI Appendix*, Fig. S2*A*). This observation suggests that C113 in LC3B is critical to binding to BRUCE.

The proteasome activator PA28γ binds to the 20S proteasome's outer (α) ring and increases entry of peptides into the particles (7). PA28γ has been shown to promote the ubiquitin-independent degradation of several nuclear proteins by proteasomes (19). PA28γ is also found in the cytoplasm (19) and has been reported to inhibit autophagy by promoting the ubiquitin-independent degradation of SirT1 (20). We found that overexpression of BRUCE in 293T cells promoted not only the degradation of endogenous LC3-I, but also the degradation of hemagglutinin-tagged LC3B, the precursor of LC3-I (*SI Appendix*, Fig. S2 *B* and *C*). We also studied a tagged version of LC3B containing a mutation at G120A, which prevents its conversion into LC3-II (9). This mutation abolished the BRUCE-induced degradation of LC3B (*SI Appendix*, Fig. S2*C*). This degradation of the cytoplasmic LC3-I required PA28γ, since deletion of PA28γ dramatically slowed the degradation of LC3-I (Fig. 1*I*). Like PA28γ, PA200 binds to the 20S proteasome's outer ring and can stimulate the ubiquitin-independent degradation of some proteins (e.g., the core histones) (21). However, deletion of PA200 deletion did not affect LC3-I degradation (Fig. 1*I*).

Bafilomycin A1 (Baf A1) is an inhibitor of lysosomal and endosomal acidification that blocks the fusion of autophagosomes with endosomes or lysosomes (8). Treatment with Baf A1 resulted in markedly increased LC3-II levels, whether or not BRUCE was knocked down (*SI Appendix*, Fig. S2*D*). Thus, BRUCE seems to inhibit autophagy by suppressing autophagosome formation rather than by influencing autolysosome function. These results imply that BRUCE inhibits autophagosome formation and autophagy by promoting PA28γ-dependent proteasomal degradation of LC3-I.

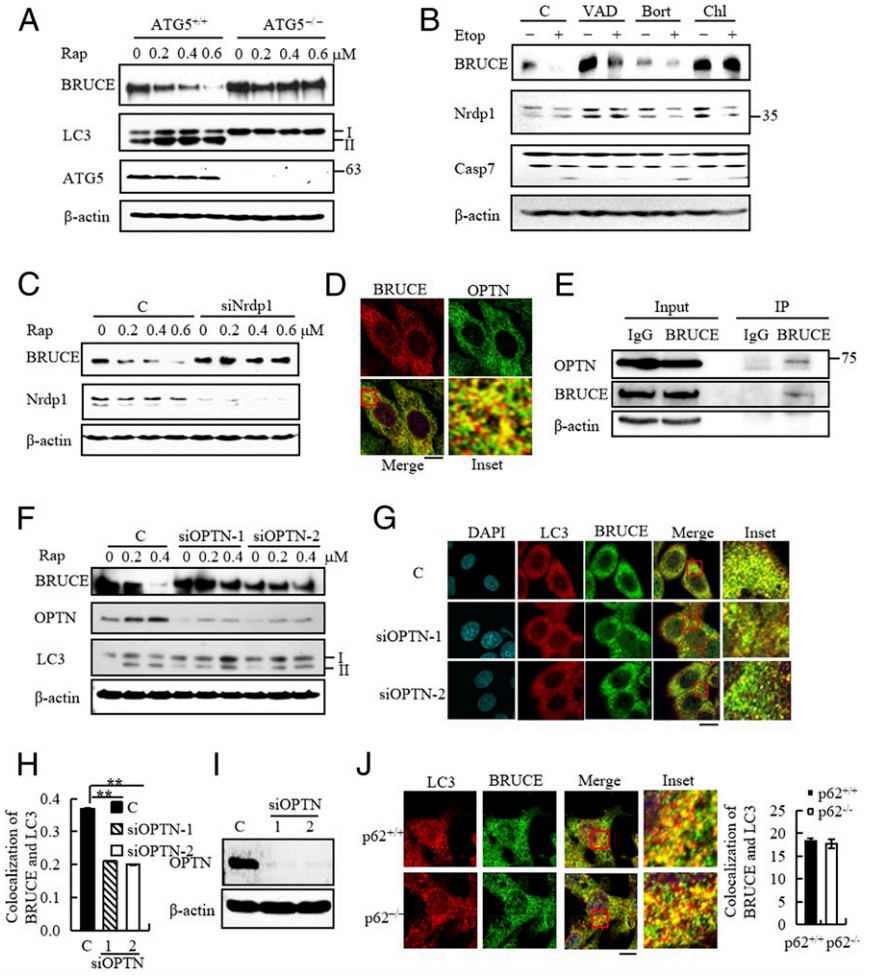

Fig. 2. Autophagic degradation of BRUCE is mediated by Nrdp1 and OPTN. (*A*) BRUCE levels in the WT or Atg5$^{-/-}$ MEFs treated with rapamycin as indicated for 24 h. (*B*) Degradation of BRUCE in MEFs treated with 20 μM etoposide (Etop) for 24 h in the presence of bortezomib (100 nM), VAD (20 μM), or chloroquine (100 μM) for 12 h. (*C*) BRUCE levels in MEFs infected with the lentivirus encoding a control RNA or siRNA for Nrdp1 and then treated with rapamycin (Rap) for 24 h. (*D*) Immunostaining of BRUCE and OPTN in HeLa cells. (Scale bar: 10 μm.) (*E*) Coimmunoprecipitation of BRUCE with OPTN in the 293T cells. (*F*) Suppression of the rapamycin-induced BRUCE degradation by OPTN knockdown. OPTN was knocked down by siRNA-oligos in HeLa cells, and treated with rapamycin as indicated for 24 h. (*G–I*) Reduced colocalization of LC3 with BRUCE in HeLa cells transfected with OPTN siRNA oligos and starved for 2 h. Protein colocalization (yellow puncta) was visualized by immunostaining (*G*) and quantified (*H*). (*I*) Efficiency of OPTN knockdown was monitored by immunoblotting (Scale bar: 10 μm). (*J*) Immunostaining of the WT or p62-deficient MEFs following starvation for 2 h (Scale bar: 10 μm.) Protein levels were analyzed by immunoblotting. Data are representative of 1 experiment with 2 independent biological replicates. Data are mean ± SEM. $n = 20$ images in *H* and *J*. $^{**}P < 0.01$, 2-tailed unpaired *t* test.

Interaction of BRUCE with SIP. BRUCE can be degraded by proteasomes or caspases on initiation of apoptosis (5). Because the BRUCE ortholog in *Drosophila*, dBRUCE, undergoes autophagic degradation before cell death in the ovary (22), we tested whether a similar mechanism functions in mammalian cells. When autophagy was induced with rapamycin or starvation by depletion of serum, glucose, and amino acids, BRUCE levels decreased (*SI Appendix*, Fig. S2 *E* and *F*). Although these treatments can also induce ubiquitination and proteasomal degradation of some proteins (23), they caused BRUCE breakdown by autophagy, since deletion of ATG5 prevented this reduction in BRUCE (Fig. 2*A*), as did treatment with chloroquine (Fig. 2*B*). In contrast, the loss of BRUCE induced by the topoisomerase inhibitor etoposide, which triggers apoptosis (5), was decreased by treatment with bortezomib or the caspase inhibitor Z-VAD-fmk (Fig. 2*B*).

This autophagic decrease in BRUCE content on treatment with rapamycin required Nrdp1, since knockdown of Nrdp1 blocked the reduction in its levels (Fig. 2*C*). Surprisingly, this degradation of BRUCE seems to involve autophagy and not the proteasome. OPTN and p62/SQSM1 are homologous proteins that bind the ubiquitinated proteins and promote their autophagic degradation by associating with LC3/GABARAP family members on the autophagosome (24). OPTN can also mediate cargo degradation in a ubiquitin-independent manner (25). OPTN, but not p62, was

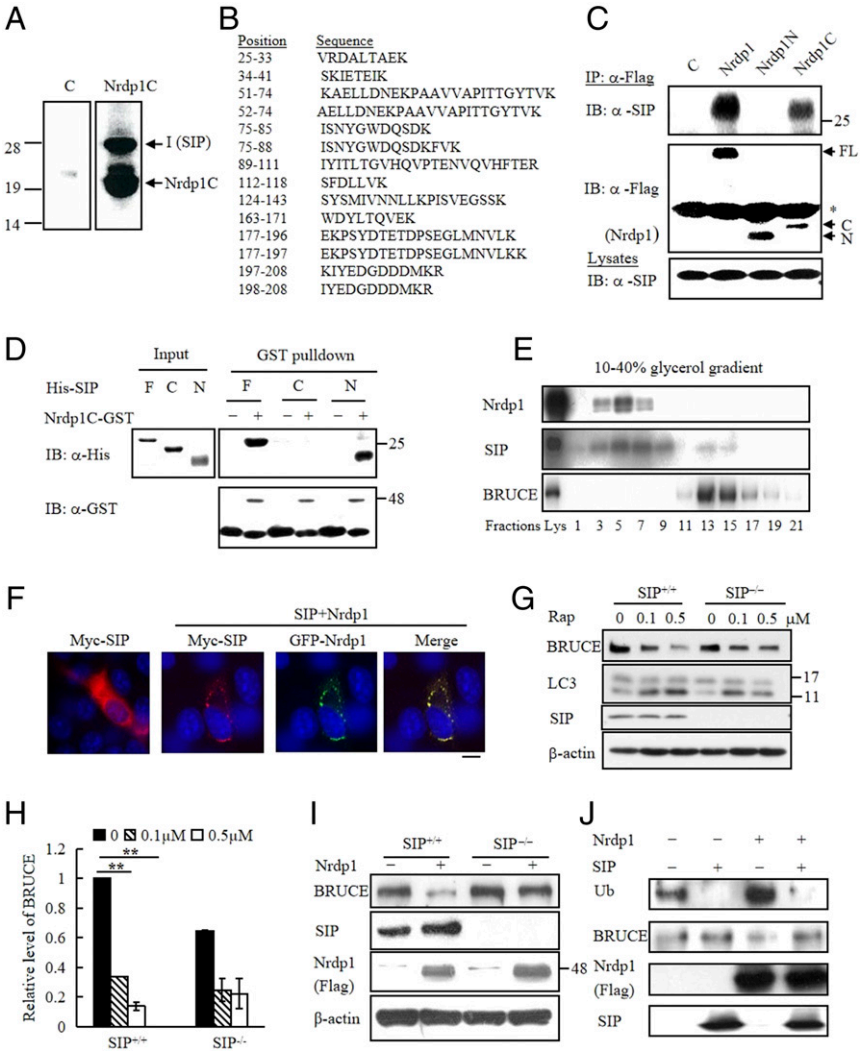

Fig. 3. SIP promotes autophagic degradation of BRUCE and inhibits BRUCE ubiquitination by competitively binding Nrdp1. (*A*) Immunoprecipitation from 293T cells transfected with an empty vector or the vector encoding the Flag-tagged C-terminal region of Nrdp1 (Nrdp1C). Following immunoprecipitation with an anti-Flag antibody and separation by SDS/PAGE, band I on the gel was characterized by mass spectrometry. This figure is a part of the image with all the proteins in figure 1A of our previous paper, where a band at 28 kDa (i.e., the band for SIP in this study) was denoted by an asterisk (6). (*B*) Sequences of 14 peptides from band I in *A* matched that for SIP/CacyBP following mass spectrometry analysis. (*C*) Immunoprecipitation following the transfection of 293T cells with the vector encoding the full-length, N-terminal region, or C-terminal region of Nrdp1. The asterisk denotes a nonspecific band. (*D*) Pulldown of SIP with Nrdp1. His-tagged SIP protein or its truncated form was incubated with the GST-fused C-terminal region of Nrdp1 and was analyzed by immunoblotting following GST pulldown assays. (*E*) Cosedimentation of SIP with Nrdp1 and BRUCE during glycerol-gradient ultracentrifugation. (*F*) Colocalization of Myc-SIP with GFP-Nrdp1 in the NIH 3T3 cells following transfection with Myc-tagged SIP and/or GFP-Nrdp1 as visualized by immunostaining ($n = 20$ images). (*G*) BRUCE levels in the WT or SIP$^{-/-}$ MEFs treated with rapamycin as indicated for 24 h. (*H*) The levels of BRUCE in *G* quantified by ImageJ (normalized to β-actin; mean ± SEM). (*I*) BRUCE levels in the WT or SIP$^{-/-}$ MEFs transfected with an empty vector or the vector encoding Flag-Nrdp1. (*J*) Inhibition of BRUCE ubiquitination by SIP. BRUCE on beads immunopurified from 293T cells was incubated with the lysates of 293T cells transfected with Nrdp1 in the presence or absence of SIP. Ubiquitination of BRUCE was detected using anti-Ub antibodies. Protein levels were analyzed by immunoblotting. Data are mean ± SEM and are representative of 1 experiment with at least 2 independent biological replicates. $^{**}P < 0.01$, 2-tailed unpaired *t* test.

required for the translocation of BRUCE into autophagosomes in the cells treated with rapamycin or on starvation (Fig. 2 *D–J* and *SI Appendix*, Fig. S2*G*). Thus, autophagic degradation of BRUCE requires both Nrdp1 and OPTN, which most likely helps deliver BRUCE to the autophagosome. Despite the requirement for Nrdp1 and OPTN for autophagic degradation of BRUCE, we were unable to detect any ubiquitination of BRUCE during its translocation into autophagosomes (data not shown), in contrast to its proteasomal degradation, where Nrdp1 clearly promotes BRUCE ubiquitination (6).

In a previous attempt to identify the Nrdp1-interacting proteins, we had found a band at ∼28 kDa in the complex that coimmunoprecipitated with the C-terminal region of Nrdp1 (6). On mass spectrometry, we identified this 28-kDa band as SIP/CacyBP (Fig. 3 *A–C*). GST-pulldown assays revealed that SIP could directly bind to Nrdp1 via its N-terminal region (Fig. 3*D*). Furthermore, glycerol-gradient ultracentrifugation and immunostaining demonstrated that SIP associated with BRUCE in addition to Nrdp1 in cells (Fig. 3 *E* and *F* and *SI Appendix*, Fig. S3 *A–C*).

Studies were then undertaken to clarify the functional importance of the SIP-Nrdp1-BRUCE interactions. Deletion of SIP in MEFs suppressed the starvation- or rapamycin-induced autophagic degradation of BRUCE (Fig. 3 *G* and *H* and *SI Appendix*, Fig. S3*D*). In contrast to the results in wild-type (WT) cells (Fig. 2*B*), both chloroquine and Baf A1 had almost no effect on the etoposide-induced degradation of BRUCE in the SIP-deficient MEFs (*SI Appendix*, Fig. S3*E*). Thus, SIP appears to be essential for the degradation of BRUCE by autophagy in the WT cells. Furthermore, deletion of SIP markedly suppressed the Nrdp1-mediated reduction of BRUCE levels (Fig. 3*I*), and the addition of SIP inhibited the in vitro ubiquitination of BRUCE by purified Nrdp1 (Fig. 3*J*), apparently because SIP reduces the binding of Nrdp1 to BRUCE. Accordingly, the purified SIP or its N-terminal region alone could reduce the coimmunoprecipitation of BRUCE with the C-terminal region of Nrdp1 (*SI Appendix*, Fig. S3*F*). Thus, SIP is required for the autophagic degradation of BRUCE on starvation or DNA damage and inhibits BRUCE ubiquitination by Nrdp1, probably by competitively decreasing the binding of Nrdp1, which mediates proteasomal degradation of BRUCE on initiation of apoptosis (6).

Promotion of Autophagy by SIP. We next examined whether SIP also regulates LC3-I degradation and autophagy. Deletion or knockdown of SIP reduced the levels of both LC3-I and LC3-II and increased the levels of p62, the accumulation of which usually indicates a decrease in autophagy, during which p62 is degraded (26) (Fig. 4 *A* and *B* and *SI Appendix*, Fig. S4*A*). These observations suggest that SIP increases autophagosome formation. Accordingly, treatment with Baf A1 markedly increased the LC3-II levels in both WT and the SIP-deficient MEFs, even though the magnitude of this increase in the SIP-deficient cells was smaller than that in the WT cells, probably because of the lower basal levels of LC3-II in the SIP-deficient cells (Fig. 4*A*). In the starved MEFs, deletion of SIP reduced the number of autophagosomes, as quantified by electron microscopy and immunostaining (Fig. 4*C* and *SI Appendix*, Fig. S4 *B–D*), but we found no difference in autophagosome size between the WT and the SIP-deficient cells. Because the fluorescence of GFP is sensitive to low pH, the GFP fluorescence of RFP-GFP-LC3B^{+} autophagosomes is quenched on their fusion with lysosomes, and

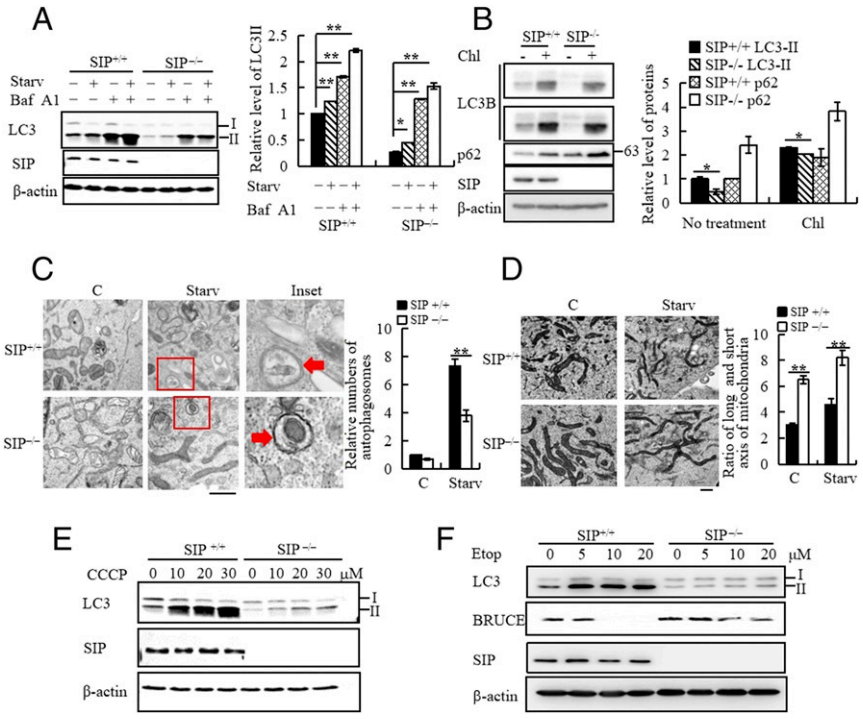

Fig. 4. SIP promotes autophagy. (*A*) Inhibition of LC3-II degradation by Baf A1. Immunoblotting of the lysates from WT or SIP$^{-/-}$ MEFs treated with 100 nM of bafilomycin A1 (Baf A1) and starvation for 2 h. LC3-II levels were quantified by ImageJ (normalized to β-actin). (*B*) Immunoblotting of the lysates from WT or SIP$^{-/-}$ MEFs treated with 10 μM chloroquine (Chl) for 24 h. The levels of LC3 and p62 were quantified by ImageJ (normalized to β-actin). (*C*) Autophagosome formation in WT or SIP$^{-/-}$ MEFs treated with starvation for 2 h. Autophagosomes were quantitated under an electron microscope. Red arrows point to autophagosomes (Scale bar: 1 μm). (*D*) Deletion of SIP leads to mitochondrial fusion. The MEFs were treated as in *C*, and the ratio of long/short axis of mitochondria were measured under an electron microscope. (Scale bar: 1 μm.) (*E*) Immunoblotting of LC3 from WT or SIP$^{-/-}$ MEFs treated with CCCP for 4 h. (*F*) Deletion of SIP attenuates the etoposide-induced formation of autophagosomal LC3-II. The WT and SIP$^{-/-}$ MEFs were treated with etoposide for 24 h at the indicated concentrations. Protein levels in *A* and *B* were analyzed by immunoblotting. Data are mean ± SEM and are representative of 1 experiment with at least 2 independent biological replicates. $n = 20$ images in *C*, $n = 800$ mitochondria in *D*. $^{*}P < 0.05$; $^{**}P < 0.01$, 2-tailed unpaired t test.

the extent of quenching can be used to monitor lysosomal fusion (8). When this approach was used in starving cells, deletion of SIP did not affect formation of the autolysosome (ratio of red vs. yellow puncta) (*SI Appendix*, Fig. S4 *D*, *Lower*). On the other hand, overexpression of SIP or a K14R mutant of SIP (described below) increased the levels of both LC3-I and LC3-II (*SI Appendix*, Fig. S4*E*). Because LC3-II is derived from LC3-I, we studied the effects on LC3-I breakdown. Knockdown of SIP promoted LC3-I degradation even in the ATG5-deficient MEFs, and this process could be blocked by bortezomib (*SI Appendix*, Fig. S4*F*). Therefore, the LC3-I degradation induced by SIP knockdown must be catalyzed by proteasomes.

After deletion of SIP, several other indications of insufficient autophagy were also evident. In the SIP-deficient cells, there was a higher ratio of long axes to short axes of mitochondria, a sign of mitochondrial fusion (27) (Fig. 4*D*). This appearance of aberrant mitochondria suggested a failure of mitophagy. To test this possibility, we used carbonyl cyanide-m-chlorophenylhydrazone (CCCP), which suppresses mitochondrial fusion and stimulates mitochondrial degradation in autophagosomes in a process termed mitophagy (28). Treatment with CCCP caused increases in the levels of LC3B-II and other LC3 family members, and deletion of SIP reduced their accumulation. SIP deletion also blocked the degradation of mitochondrial membrane proteins Tom20 and Tim23, which occurs during mitophagy (27) (Fig. 4*E* and *SI Appendix*, Fig. S4 *G* and *H*). In addition, the deletion of SIP attenuated the etoposide-induced formation of LC3B-II and other LC3 family members (Fig. 4*F* and *SI Appendix*, Fig. S4*I*). Conversely, the addition of Baf A1 increased the levels of LC3B-II and other LC3 family members in both the WT and the SIP-deficient MEFs after treatment with CCCP or etoposide (*SI Appendix*, Fig. S4 *H* and *I*). Because Baf A1 blocks the fusion of autophagosomes with endosomes or lysosomes (8), these results provide further evidence indicating that SIP promotes autophagosome formation.

Autophagy is also important in the clearance of aggregates of misfolded proteins, which accumulate in many proteotoxic diseases (28, 29). For example, Huntington's disease is caused by the toxic accumulation of polyglutamine aggregates of mutant huntingtin (Htt) containing an expanded polyQ sequence (Htt-polyQ). Therefore, we studied the effects of SIP knockdown on the levels of mutant Htt with a 74-glutamine repeat (Htt-74Q) (*SI Appendix*, Fig. S4*J*). Loss of SIP in HEK293T cells led to a further buildup of the mutant Htt. Thus, SIP promotes autophagosome formation and the autophagic degradation of mitochondria and polyQ aggregates.

SIP-Mediated Translocation of BRUCE. The GTPase Rab8, localized in part at the Golgi apparatus and in part on early endosomes, seems to regulate cargo transport from the trans-Golgi network to recycling endosomes (30). As reported previously (31), BRUCE colocalized with the ectopically expressed GFP-Rab8 in HeLa cells (*SI Appendix*, Fig. S5*A*). In addition, the transfected Nrdp1 colocalized with GFP-Rab8 (*SI Appendix*, Fig. S5*B*). Furthermore, cotransfection of Nrdp1 or treatment with etoposide increased the amount of SIP colocalized with GFP-Rab8 or endogenous Rab8 (Fig. 5 *A* and *B* and *SI Appendix*, Fig. S5 *C–F*). Coimmunoprecipitation assays also indicated that etoposide stimulated the association of SIP with Rab8 (*SI Appendix*, Fig. S5 *G* and *H*); however, deletion of SIP had no effect on the colocalization of BRUCE with Rab8 in HeLa cells (*SI Appendix*, Fig. S5*I*). Furthermore, LC3-I, but not LC3-II, was detectable in the Rab8-BRUCE complex (Fig. 5*C*). Knockdown of Rab8 dramatically reduced the colocalization of LC3-II with BRUCE in the MEFs treated with rapamycin (Fig. 5 *D* and *E* and *SI Appendix*, Fig. S5*J*), suggesting that Rab8 is important for translocation of BRUCE into the autophagosome. Thus, both up-regulation of Nrdp1 and treatment with etoposide promote the association of SIP with Rab8, BRUCE, and LC3-I in the trans-Golgi network.

Rab11 is found predominantly in the recycling endosome, which contributes to the formation of autophagosomes (32). BRUCE could also be coimmunoprecipitated with Rab11 and LC3-I, especially following etoposide treatment (Fig. 5 *F* and *G*). Both BRUCE and Flag-Nrdp1 colocalized with the transfected GFP-Rab11 (*SI Appendix*, Fig. S5 *K* and *L*). Deletion of SIP markedly reduced this colocalization and the interaction of BRUCE with Rab11 in MEFs (Fig. 5*H* and *SI Appendix*, Fig. S5*M*). Furthermore, knockdown of Rab11 reduced the colocalization of BRUCE and LC3-II in autophagosomes (Fig. 5 *I* and *J* and *SI Appendix*, Fig. S5*N*). Because conversion of LC3-I into LC3-II occurs during the formation of autophagosomes (8), SIP seems to be required for the translocation of BRUCE and LC3-I from the trans-Golgi network to the recycling endosome, and it eventually contributes to the formation of the autophagosome (32).

Monoubiquitination of SIP on DNA Damage Reduces Autophagy but Promotes Apoptosis. In studies aimed at further clarifying the cellular role of SIP, we found that on treatment with the topoisomerase inhibitor camptothecin or etoposide, SDS/PAGE revealed a slower-migrating species of SIP that seemed to be 6–8 kDa larger (Fig. 6*A* and *SI Appendix*, Fig. S6*A*). This species was identified by immunoblotting as a monoubiquitinated form of SIP, which increased in amount after camptothecin treatment or transfection of Nrdp1 (Fig. 6 *B* and *C* and *SI Appendix*, Fig. S6 *B* and *C*). By screening the ubiquitination sites of SIP, we found that the K14R mutation of SIP could abolish the Nrdp1-mediated ubiquitination of SIP (Fig. 6*C*). As shown above (*SI Appendix*, Fig. S3*F*), deletion of SIP reduced the etoposide-induced degradation of BRUCE by autophagy, as shown by its decreased inhibition by chloroquine (Fig. 6*D*). When we expressed the WT SIP or its K14R mutant ectopically in the SIP-deficient MEFs, we found that both could restore the sensitivity to chloroquine (Fig. 6*D*).

Deletion of SIP also led to a dramatic increase in levels of the active caspase 3 in MEFs (Fig. 6*D*), but expression of either the WT SIP or its mutant sharply reduced the etoposide-induced activation of caspase 3 and apoptosis (Fig. 6*D* and *SI Appendix*, Fig. S6 *D–F*). However, in the presence of chloroquine, the levels of active caspase 3 were much lower in the cells transfected with the mutant SIP compared with those transfected with the WT SIP (Fig. 6*D*), probably because inhibition of lysosomal activity prevented the autophagic degradation of BRUCE, and the loss of SIP monoubiquitination eventually allowed BRUCE to inhibit caspase activation. Thus, monoubiquitination of SIP appears to switch the cellular response to these DNA-damaging agents from stimulating autophagy to inducing apoptosis.

Discussion

The present studies have identified several factors and mechanisms that regulate autophagy as well as apoptosis in mammalian cells (Fig. 6*E*). Central in these mechanisms is BRUCE, whose importance as an IAP in inhibiting apoptosis had been demonstrated previously (5). BRUCE was shown here to reduce the cellular levels of LC3-I by promoting its degradation by proteasomes and thereby also decreasing the levels of LC3-II and autophagy. The relative importance of these 2 actions of BRUCE in suppressing autophagy and in inhibiting apoptosis may depend simply on its cellular concentration, but may also be a point of further regulation. When BRUCE was knocked down using a lentiviral infection of siRNA, autophagy became activated 3 d later and apoptosis 4 d thereafter. The reason for the greater lag time for apoptosis is perhaps because the induction of apoptosis requires a greater drop in BRUCE content. These effects of BRUCE on LC3-I, but not on LC3-II degradation, have

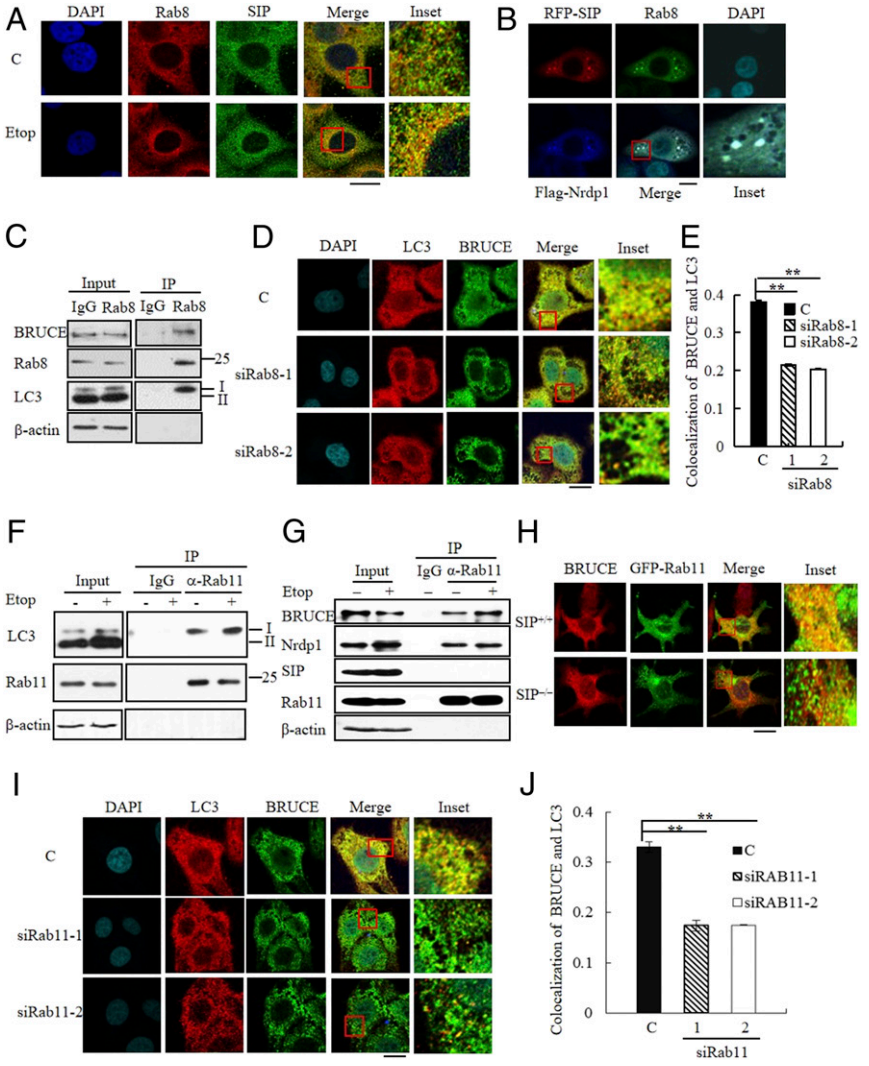

Fig. 5. SIP promotes the translocation of BRUCE and LC3-I to autophagosomes. (*A*) Etoposide (Etop) stimulates colocalization of Rab8 with SIP as analyzed by immunostaining of HeLa cells treated with mock (C) or 20 μM Etop for 24 h. (*B*) Nrdp1 promotes colocalization of Rab8 with SIP as analyzed by immunostaining of the HeLa cells transfected with Flag-Nrdp1 and RFP-SIP. White puncta indicate triple colocalization of proteins. (*C*) Coimmunoprecipitation of Rab8 with LC3-I and BRUCE from HeLa cell lysates. (*D*) HeLa cells were transfected with siRNA-oligos for Rab8, starved for 2 h, and then analyzed by immunostaining. (*E*) Colocalization of BRUCE with LC3 in *D* was quantified using ImageJ. (*F*) Coimmunoprecipitation of Rab11 with LC3-I from HeLa cell lysates. (*G*) Coimmunoprecipitation of Rab11 with BRUCE and Nrdp1 in the 293T cells treated with 0 or 20 μM etoposide for 24 h. (*H*) Deletion of SIP reduces colocalization of BRUCE with GFP-Rab11 in the MEFs transfected with GFP-Rab11 and starved for 2 h as visualized by immunostaining. (*I*) HeLa cells were transfected with siRNA oligos for Rab11 and starved for 2 h. Protein localization was assayed by immunostaining. (*J*) Colocalization between BRUCE and LC3 in *I* was quantified by ImageJ. Data are mean ± SEM, representative of 1 experiment with 2 independent biological replicates. Protein levels in *C*, *F*, and *G* were analyzed by immunoblotting. $n = 20$ images. $^{**}P < 0.01$, 2-tailed unpaired t test. (Scale bar: 10 μm.)

provided an unexpected additional mechanism underlying the physiological suppression of autophagy under normal conditions. It is interesting that another important inhibitor of apoptosis, XIAP, which also functions as a ubiquitin ligase, has been shown to inhibit autophagy, although by a very different mechanism (33).

Under normal conditions, these inhibitory actions of BRUCE seem to be enhanced by SIP, which protects it from ubiquitination by Nrdp1 and proteasomal degradation (6). As shown here, SIP and BRUCE associate with each other, and the bound SIP seems to prevent Nrdp1 from binding BRUCE and catalyzing its degradation. However, prolonged exposure of cells to the topoisomerase inhibitors not only induced Nrdp1-mediated degradation of BRUCE (6), but also caused the monoubiquitination of SIP by Nrdp1. This change in Nrdp1's catalytic behavior with different substrates (i.e., from chain formation for proteasomal targeting to monoubiquitination) is interesting mechanistically and has important consequences. As a result, SIP together with Nrdp1 promotes autophagosome formation and BRUCE degradation by autophagy.

Autophagy can be activated by many factors, including starvation for nutrients and DNA damage (14, 22, 34–36), which act through distinct mechanisms. Exactly how these known regulators of autophagy (especially mTOR and ULK1) impact these BRUCE or SIP-dependent mechanisms, and how these proteins may influence the autophagy activation by mTOR inhibition of nutrient deprivation, will be important issues for future study. The changes in SIP-mediated autophagy observed here with rapamycin or starvation suggest that these actions of SIP and BRUCE degradation are somehow linked to the regulation of autophagy by mTOR. However, our experiments have revealed a quite different mechanism for regulating autophagy under normal conditions by

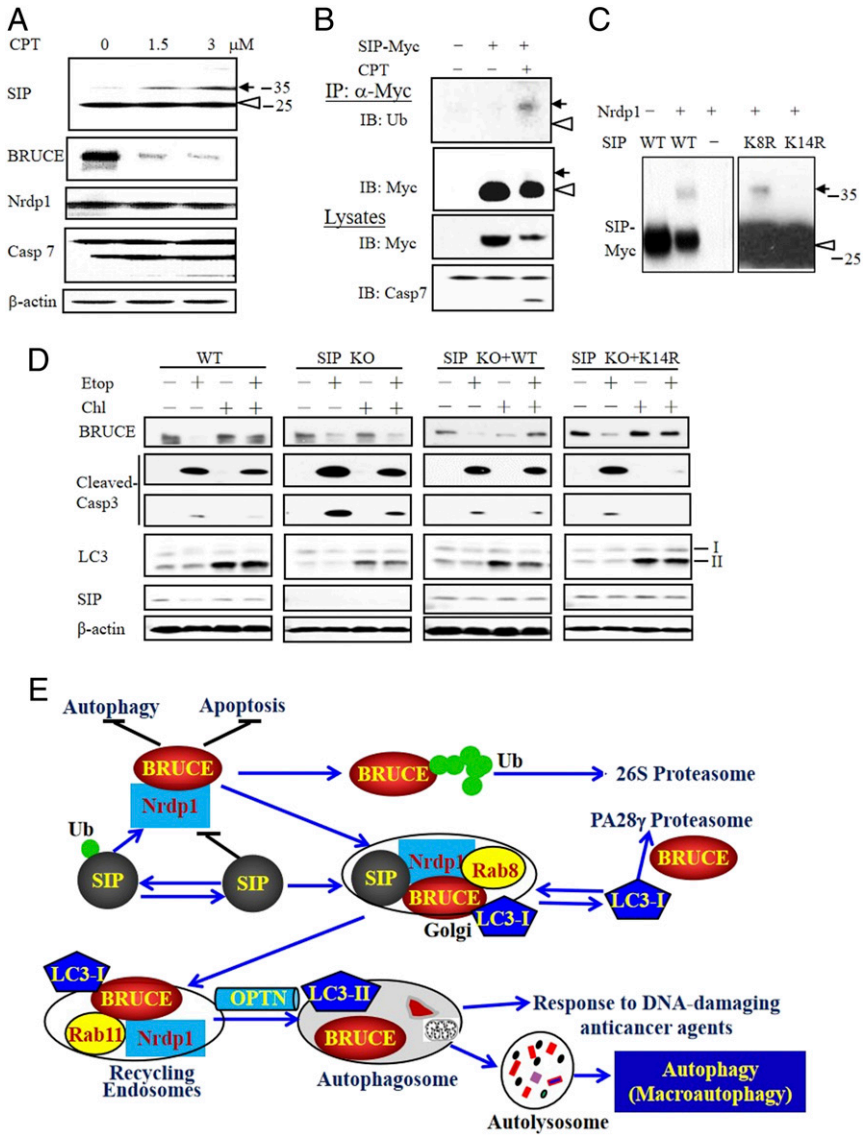

Fig. 6. SIP serves as a switch between apoptosis and autophagy. (*A*) Induction of a slower-migrating species in MDA-MB-453 cells treated with CPT as indicated for 24 h. (*B*) Identification of monoubiquitinated SIP in the MDA-MB-468 cells transfected with Myc-SIP and treated with 3 μM CPT. Myc-SIP was immunoprecipitated. (*C*) Mutation of SIP at K14R eliminates monoubiquitination of SIP in 293T cells transfected with Flag-Nrdp1 and/or Myc-SIP or its mutant. (*D*) Mutation of SIP at K14R reduces the etoposide-induced activation of caspase 3 in the $SIP^{-/-}$ MEFs (SIP KO) stably transfected with SIP (WT) or its K14R mutant and treated with 40 μM etoposide for 24 h and/or 100 μM chloroquine for 12 h. (*E*) Summary of the present findings about how SIP promotes autophagy by promoting the degradation of BRUCE/Apollon and LC3-I. Protein levels in *A*–*D* were analyzed by immunoblotting. The open triangle and arrow in *A*–*C* indicate SIP and its monoubiquitinated form, respectively.

promoting proteasomal degradation of LC3-I. Because BRUCE binds LC3-I, it is possible that BRUCE directly ubiquitinates LC3-I through its capacity to act as an E2 and E3, although we were unable to obtain direct evidence for ubiquitination of LC3-I. Surprisingly, the breakdown of LC3-I was also found to require PA28γ, which has been shown to promote the degradation of certain proteins by the 20S proteasome in a process not requiring ubiquitination (13). However, PA28γ in cells can also associate with singly capped 26S proteasomes to form hybrid complexes (19S-20S-PA28γ) that can facilitate the breakdown of ubiquitinated proteins (7). In addition, PA28γ also closely associates with PIP30, which alters its interactions in vivo (37). A full understanding of this intriguing requirement for PA28γ and BRUCE action will require further in-depth study.

After the present study was completed, Ebner et al. (38) also showed, but by a quite different approach, a role for BRUCE in inhibiting autophagy by reducing autophagosome-lysosome fusion, which may be a consequence of the reduction in LC3-II levels demonstrated here. The authors also reported that exogenously expressed BRUCE associates preferentially with GABARAP and GABARAPL1 (38). The spectrum of LC3/GABARAP family members associated with BRUCE in their study differed somewhat from that reported here, perhaps due to insufficient extraction from cells of the membrane-associated BRUCE in their pull-down experiments (6, 31). In contrast, we used the soluble GST-LIR motif of BRUCE to ensure efficient interactions with the LC3/GABARAP family members. We also found that BRUCE bound GABARAP, GABARAPL1, and GABARAPL2, although more weakly than LC3B. BRUCE promoted the degradation of GABARAP, although whether this effect occurred via changes in LC3B is unclear. Although LC3-I and LC3-II have been reported to be degraded by the purified 20S proteasomes (39),

many proteins show such a sensitivity in vitro but are degraded by other mechanisms in cells. In fact, it is very well documented that LC3-II is degraded together with the contents of autophagosomes after fusion with lysosomes (8).

To catalyze ubiquitination and proteasomal degradation of BRUCE during apoptosis, Nrdp1 must form a ubiquitin chain on BRUCE (6). In contrast, Nrdp1 was shown here to catalyze monoubiquitination of SIP. Although the very large size of BRUCE precluded a judgment, it is possible that BRUCE was also monoubiquitinated. Monoubiquitination of SIP clearly plays a critical role in altering the activities and subcellular localization of both SIP and BRUCE and leads to activation of multiple autophagic processes, including clearance of damaged mitochondria and aggregates of mutant Htt with an expanded polyglutamine sequence. Interestingly, Nrdp1 reportedly also affects autophagy and mitophagy through interaction with the Clec16a protein, a membrane-associated endosomal protein. The Clec16a gene has been implicated in type 1 diabetes and multiple other immune-mediated diseases, including multiple sclerosis. Nrdp1 appears to function with Clec16a and the ubiquitin ligase Parkin in marking damaged mitochondria for autophagic degradation (40, 41).

This study also uncovered another mechanism promoting BRUCE degradation, in which BRUCE is switched from being an inhibitor of autophagy to a substrate (Fig. 6*E*). Nrdp1 promoted the translocation of SIP into the trans-Golgi network and the SIP-dependent translocation of BRUCE into the recycling endosome, which eventually led to greater autophagosome formation and autophagy. This translocation of BRUCE from the recycling endosome into the autophagosome also required OPTN, which delivers cargoes, especially ubiquitinated proteins, to the autophagosome by binding to LC3 proteins. Because OPTN functions as a ubiquitin receptor, and because Nrdp1 initiated this process, a role for ubiquitination seemed likely, although we have been unable to demonstrate a ubiquitin requirement or involvement of the E2 activity of BRUCE in this process (unpublished observations). The involvement of OPTN is also intriguing because OPTN mutations and defects in autophagy have been implicated in some forms of amyotrophic lateral sclerosis (42) and glaucoma (43). Through these changes in BRUCE localization under stressful conditions (e.g., DNA damage), SIP not only raises LC3-I levels and promotes autophagic degradation of BRUCE, but also enhances the clearance of Htt-polyQ aggregates and damaged mitochondria. The actual importance of these mechanisms in activating autophagy or cell death in different cell types will be important to study under various physiological and pathological conditions.

Materials and Methods

Cell Culture and Treatments. MDA-MB-453, 293T, HeLa, and COS7 cells were cultured in DMEM supplemented with 10% FBS, 100 U/mL penicillin, and 100 μg/mL streptomycin. MEFs were cultured in this medium supplemented with 1% nonessential amino acids and 200 μM β-mercaptoethanol. All cells were kept at 37 °C in 5% CO_2. Cell starvation was performed by incubating cells in Dulbecco's PBS medium at 37 °C in 5% CO_2 after 2 washes with PBS. Dulbecco's PBS medium is a balanced salt solution with the following components: 2.67 mM KCl, 1.47 mM KH_2PO_4, 137.93 mM NaCl, and 8.06 mM Na_2HPO_4-$7H_2O$.

Cell Transfection or Infection. Cells were plated in growth medium (with or without antibiotics) at 1 d before transfection so that they would be 70–90% confluent at the time of transfection. DNA or siRNA oligos and LipoMax (Sudgen Biotechnology) were diluted in Opti-MEM and incubated for 5 min at room temperature, respectively. Then the 2 solutions were mixed, followed by a 20-min incubation at room temperature. Finally, the complex was added into a plate and incubated with the cells at 37 °C in a CO_2 incubator for 24–48 h. The infection of cells with viruses was performed in the presence of polybrene following virus packaging by transfection and concentration by ultracentrifugation.

Immunostaining and Apoptosis Assays. These assays were carried out as described previously (21). In brief, cells on glass coverslips in 6-well plates were fixed in 4% polyformaldehyde for 10 min at room temperature, followed by membrane permeation using 100 μg/mL digitonin in PBS for 5 min. Cells were blocked in 3% BSA before primary antibodies were applied. Primary antibodies were incubated in a moist container at room temperature for 1 h. Then the secondary antibodies conjugated with FITC, Cy5, or Alexa Fluor 594 were applied to the cells in a moist container at room temperature for 1 h. Apoptotic DNA fragmentation was analyzed using the DeadEnd Fluorometric TUNEL System according to the standard paraffin-embedded tissue section protocol (Promega). The DNAs in nuclei were stained with DAPI at the final preparation step. The slides were viewed on a Zeiss LSM 700 confocal microscope using a 100× oil objective and laser at 488, 555, or 639 nm for excitation.

Immunoblotting Assay. Cell lysis was carried out by sonication in the lysis buffer containing 20 mM Tris·HCl pH 8.0, 100 mM KCl, 0.2% Nonidet P-40, 10% glycerol, 1 mM $ZnCl_2$, 10 mM β-glycerophosphate, 5 mM tetrasodium pyrophosphate, 1 mM NaF, 1 mM Na_3VO_4, and a protease inhibitor mixture. Protein samples were separated by SDS/PAGE and transferred onto PVDF membranes. Antibodies or antisera specific proteins were used as primary antibodies to detect the corresponding proteins. Peroxidase-conjugated anti-mouse IgG (1:5,000), anti-rat IgG (1:4,000), or anti-rabbit IgG (1:3,000) was used as the secondary antibody. The protein bands were visualized by an ECL detection system (EMD Millipore) or Odyssey imaging system (LI-COR).

Electron Microscopy. Cells were first fixed with 2.5% glutaraldehyde in Na cacodylate buffer (pH 7.4) at 37 °C for 2 h, dehydrated in a graded ethanol series, and embedded in Epon 812. The samples on 100-nm sections were visualized using a JEOL electron microscope at 80 kV, and images were captured using an AMT digital camera.

Immunoprecipitation. Cells were lysed with the lysis buffer as in the immunoblotting procedure, and the lysates were immunoprecipitated with specific antibody and protein A/G-Sepharose (Sigma-Aldrich) at 4 °C for 2 h. The precipitants were washed 3 times with the lysis buffer, after which the immune complexes were eluted with the sample buffer containing 1× SDS at 97 °C for 6 min and then separated by SDS/PAGE.

GST Pulldown Assay. The putative LIR motif of BRUCE and its mutant were fused to GST, expressed in bacteria, and purified using standard protocols. The GST pulldown of His-LC3, which was expressed and purified from bacteria, was carried out in the buffer containing 10 mM Na-Hepes pH 7.5, 150 mM NaCl, 0.005% Tween-20, and 2 mM DTT. Then the beads were washed in the buffers containing 10 mM Na-Hepes pH 7.5, 150–300 mM KCl, 0.5–1.0% Tween-20, and 2 mM DTT.

Mass Spectrometry. 293T cells were transfected with an empty vector or the vector encoding the Flag-tagged C-terminal region of Nrdp1 (Nrdp1C), and immunoprecipitation was performed as described previously (6). The band at approximately 30 kDa was excised for analysis by mass spectrometry. The mass spectrometry analysis of protein samples was performed by MALDI-TOF using an Applied Biosystems Voyager-DE-STR Biospectrometry Workstation.

In Vitro Ubiquitination Assay. BRUCE on beads immunopurified from 293T cells was incubated with the lysates of 293T cells transfected with Nrdp1 in the presence or the absence of SIP. The reaction was carried out in the ubiquitination buffer as described previously (6). Ubiquitination of BRUCE was detected by immunoblotting using anti-Ub antibodies.

Quantification and Statistical Analysis. Unless stated otherwise, significance levels for comparisons between 2 groups were determined by one-way ANOVA. Data are reported as mean ± SEM. $*P < 0.05$; $**P < 0.01$, normal distribution. All images were chosen at random and while blinded and were quantitated using ImageJ.

ACKNOWLEDGMENTS. We thank Qimin Zhan (Peking University Health Science Center) for critical comments; Eileen White (The State University of New Jersey), Junying Yuan (Harvard Medical School), Yoshinori Ohsumi (Tokyo Institute of Technology), Masaaki Komatsu (Niigata University), Stefan Jentsch (Max Planck), Quan Chen (Chinese Academy of Sciences), Marcelo D. Gomes (University of São Paulo), Lance Barton (Austin College,) and Xiaotao Li (East China Normal University) for reagents; and Hwang-Ho Cha and Hengliang Shi for technical assistance. Funding was provided by the Ministry of Science and Technology of China (Grant 2018YFC1003303) and the National Natural Science Foundation of China (Grants 31530014, 91319303, 81825014, 31830003, and 31600626).

1. G. Mariño, M. Niso-Santano, E. H. Baehrecke, G. Kroemer, Self-consumption: The interplay of autophagy and apoptosis. *Nat. Rev. Mol. Cell Biol.* **15**, 81–94 (2014).
2. E. White, Deconvoluting the context-dependent role for autophagy in cancer. *Nat. Rev. Cancer* **12**, 401–410 (2012).
3. T. Bartke, C. Pohl, G. Pyrowolakis, S. Jentsch, Dual role of BRUCE as an antiapoptotic IAP and a chimeric E2/E3 ubiquitin ligase. *Mol. Cell* **14**, 801–811 (2004).
4. Y. Hao *et al*., Apollon ubiquitinates SMAC and caspase-9, and has an essential cytoprotection function. *Nat. Cell Biol.* **6**, 849–860 (2004).
5. X. B. Qiu, A. L. Goldberg, The membrane-associated inhibitor of apoptosis protein, BRUCE/Apollon, antagonizes both the precursor and mature forms of Smac and caspase-9. *J. Biol. Chem.* **280**, 174–182 (2005).
6. X. B. Qiu, S. L. Markant, J. Yuan, A. L. Goldberg, Nrdp1-mediated degradation of the gigantic IAP, BRUCE, is a novel pathway for triggering apoptosis. *EMBO J.* **23**, 800–810 (2004).
7. G. A. Collins, A. L. Goldberg, The logic of the 26S proteasome. *Cell* **169**, 792–806 (2017).
8. D. C. Rubinsztein *et al*., In search of an "autophagomometer". *Autophagy* **5**, 585–589 (2009).
9. Y. Kabeya *et al*., LC3, a mammalian homologue of yeast Apg8p, is localized in autophagosome membranes after processing. *EMBO J.* **19**, 5720–5728 (2000).
10. Z. Sha, A. L. Goldberg, Proteasome-mediated processing of Nrf1 is essential for coordinate induction of all proteasome subunits and p97. *Curr. Biol.* **24**, 1573–1583 (2014).
11. A. M. Topolska-Woś, W. J. Chazin, A. Filipek, CacyBP/SIP–Structure and variety of functions. *Biochim. Biophys. Acta* **1860**, 79–85 (2016).
12. S. I. Matsuzawa, J. C. Reed, Siah-1, SIP, and Ebi collaborate in a novel pathway for beta-catenin degradation linked to p53 responses. *Mol. Cell* **7**, 915–926 (2001).
13. X. Li *et al*., The SRC-3/AIB1 coactivator is degraded in a ubiquitin- and ATP-independent manner by the REGgamma proteasome. *Cell* **124**, 381–392 (2006).
14. A. Kuma *et al*., The role of autophagy during the early neonatal starvation period. *Nature* **432**, 1032–1036 (2004).
15. A. B. Birgisdottir, T. Lamark, T. Johansen, The LIR motif—Crucial for selective autophagy. *J. Cell Sci.* **126**, 3237–3247 (2013).
16. J. Yuan, B. A. Yankner, Apoptosis in the nervous system. *Nature* **407**, 802–809 (2000).
17. T. Shpilka, H. Weidberg, S. Pietrokovski, Z. Elazar, Atg8: An autophagy-related ubiquitin-like protein family. *Genome Biol.* **12**, 226 (2011).
18. M. B. Schaaf, T. G. Keulers, M. A. Vooijs, K. M. Rouschop, LC3/GABARAP family proteins: Autophagy-(un)related functions. *FASEB J.* **30**, 3961–3978 (2016).
19. Y. Wu *et al*., Regulation of REGγ cellular distribution and function by SUMO modification. *Cell Res.* **21**, 807–816 (2011).
20. S. Dong *et al*., The REGγ proteasome regulates hepatic lipid metabolism through inhibition of autophagy. *Cell Metab.* **18**, 380–391 (2013).
21. M. X. Qian *et al*., Acetylation-mediated proteasomal degradation of core histones during DNA repair and spermatogenesis. *Cell* **153**, 1012–1024 (2013).
22. I. P. Nezis *et al*., Autophagic degradation of dBruce controls DNA fragmentation in nurse cells during late Drosophila melanogaster oogenesis. *J. Cell Biol.* **190**, 523–531 (2010).
23. J. Zhao, B. Zhai, S. P. Gygi, A. L. Goldberg, mTOR inhibition activates overall protein degradation by the ubiquitin proteasome system as well as by autophagy. *Proc. Natl. Acad. Sci. U.S.A.* **112**, 15790–15797 (2015).
24. Y. C. Wong, E. L. Holzbaur, Optineurin is an autophagy receptor for damaged mitochondria in parkin-mediated mitophagy that is disrupted by an ALS-linked mutation. *Proc. Natl. Acad. Sci. U.S.A.* **111**, E4439–E4448 (2014).
25. J. Korac *et al*., Ubiquitin-independent function of optineurin in autophagic clearance of protein aggregates. *J. Cell Sci.* **126**, 580–592 (2013).
26. M. Komatsu *et al*., Homeostatic levels of p62 control cytoplasmic inclusion body formation in autophagy-deficient mice. *Cell* **131**, 1149–1163 (2007).
27. T. Goiran *et al*., Nuclear p53-mediated repression of autophagy involves PINK1 transcriptional down-regulation. *Cell Death Differ.* **25**, 873–884 (2018).
28. D. Narendra, A. Tanaka, D. F. Suen, R. J. Youle, Parkin is recruited selectively to impaired mitochondria and promotes their autophagy. *J. Cell Biol.* **183**, 795–803 (2008).
29. K. Lu, I. Psakhye, S. Jentsch, Autophagic clearance of polyQ proteins mediated by ubiquitin-Atg8 adaptors of the conserved CUET protein family. *Cell* **158**, 549–563 (2014).
30. T. Sato *et al*., The Rab8 GTPase regulates apical protein localization in intestinal cells. *Nature* **448**, 366–369 (2007).
31. C. Pohl, S. Jentsch, Final stages of cytokinesis and midbody ring formation are controlled by BRUCE. *Cell* **132**, 832–845 (2008).
32. C. Puri, M. Renna, C. F. Bento, K. Moreau, D. C. Rubinsztein, Diverse autophagosome membrane sources coalesce in recycling endosomes. *Cell* **154**, 1285–1299 (2013).
33. X. Huang, Z. Wu, Y. Mei, M. Wu, XIAP inhibits autophagy via XIAP-Mdm2-p53 signalling. *EMBO J.* **32**, 2204–2216 (2013).
34. S. Kaushik *et al*., Loss of autophagy in hypothalamic POMC neurons impairs lipolysis. *EMBO Rep.* **13**, 258–265 (2012).
35. B. Coupé *et al*., Loss of autophagy in pro-opiomelanocortin neurons perturbs axon growth and causes metabolic dysregulation. *Cell Metab.* **15**, 247–255 (2012).
36. A. M. Cuervo, Autophagy and aging: Keeping that old broom working. *Trends Genet.* **24**, 604–612 (2008).
37. B. Jonik-Nowak *et al*., PIP30/FAM192A is a novel regulator of the nuclear proteasome activator PA28γ. *Proc. Natl. Acad. Sci. U.S.A.* **115**, E6477–E6486 (2018).
38. P. Ebner *et al*., The IAP family member BRUCE regulates autophagosome-lysosome fusion. *Nat. Commun.* **9**, 599 (2018).
39. Z. Gao *et al*., Processing of autophagic protein LC3 by the 20S proteasome. *Autophagy* **6**, 126–137 (2010).
40. L. Zhong, Y. Tan, A. Zhou, Q. Yu, J. Zhou, RING finger ubiquitin-protein isopeptide ligase Nrdp1/FLRF regulates parkin stability and activity. *J. Biol. Chem.* **280**, 9425–9430 (2005).
41. S. A. Soleimanpour *et al*., The diabetes susceptibility gene Clec16a regulates mitophagy. *Cell* **157**, 1577–1590 (2014).
42. S. Nakazawa *et al*., Linear ubiquitination is involved in the pathogenesis of optineurin-associated amyotrophic lateral sclerosis. *Nat. Commun.* **7**, 12547 (2016).
43. R. P. Toth, J. D. Atkin, Dysfunction of optineurin in amyotrophic lateral sclerosis and glaucoma. *Front. Immunol.* **9**, 1017 (2018).